Unraveling the Consecutive Recombination Events in the Human *IGK* Locus[1]

Anton W. Langerak,[2]* Bertrand Nadel,† Anneke de Torbal,* Ingrid L. M. Wolvers-Tettero,* Ellen J. van Gastel-Mol,* Brenda Verhaaf,* Ulrich Jäger,† and Jacques J. M. van Dongen*

In addition to the classical Vκ-Jκ, Vκ-κ deleting element (Kde), and intron-Kde gene rearrangements, atypical recombinations involving Jκ recombination signal sequence (RSS) or intronRSS elements can occur in the Igκ (*IGK*) locus, as observed in human B cell malignancies. In-depth analysis revealed that atypical JκRSS-intronRSS, Vκ-intronRSS, and JκRSS-Kde recombinations not only occur in B cell malignancies, but rather reflect physiological gene rearrangements present in normal human B cells as well. Excision circle analysis and recombination substrate assays can discriminate between single-step vs multistep rearrangements. Using this combined approach, we unraveled that the atypical Vκ-intronRSS and JκRSS-Kde pseudohybrid joints most probably result from ongoing recombination following an initial aberrant JκRSS-intronRSS signal joint formation. Based on our observations in normal and malignant human B cells, a model is presented to describe the sequential (classical and atypical) recombination events in the human *IGK* locus and their estimated relative frequencies (0.2–1.0 vs <0.03). The initial JκRSS-intronRSS signal joint formation (except for Jκ1RSS-intronRSS) might be a side event of an active V(D)J recombination mechanism, but the subsequent formation of Vκ-intronRSS and JκRSS-Kde pseudohybrid joints can represent an alternative pathway for *IGK* allele inactivation and allelic exclusion, in addition to classical Cκ deletions. Although usage of this alternative pathway is limited, it seems essential for inactivation of those *IGK* alleles that have undergone initial aberrant recombinations, which might otherwise hamper selection of functional Ig L chain proteins. ***The Journal of Immunology*, 2004, 173: 3878–3888.**

To form a large variety of unique Ag-recognizing Ig molecules, human B cells undergo recombination between variable (V), diversity (D), and joining (J) gene segments of the Ig genes. The resulting V(D)J exons encode the variable domains of Ig chains. In the bone marrow, VDJ recombination of Ig H chain (*IGH*)[3] genes starts at the progenitor B cell stage, followed by VJ recombination in Igκ (*IGK*) or Igλ (*IGL*) L chain loci during the small precursor B cell or precursor B-II cell stage (1, 2). Pairing of Ig H and Ig κ or Ig λ-chains allows further differentiation into immature and subsequently mature surface membrane Igκ- or Igλ-positive B cells.

Previous studies have shown that most Igκ-positive B cells retain their *IGL* genes in germline configuration (3, 4). In contrast, the vast majority of Igλ-positive B cells have one or two rearranged *IGK* alleles in addition to their rearranged *IGL* allele(s), in line with hierarchical Ig L chain recombination (4, 5). In Igλ-positive B cells, the *IGK* rearrangements mainly concern deletional rearrangements involving the κ-deleting element (Kde), which is positioned downstream of the constant (Cκ) gene segment (6) (Fig. 1). Kde can either recombine to a Vκ gene segment upstream of a previously formed Vκ-Jκ rearrangement or to an isolated heptamer recombination signal sequence (RSS) in the intron between the Jκ gene segments and the Cκ exon (intronRSS heptamer) (6) (Fig. 1). Recombination to the intronRSS heptamer results in the deletion of Cκ and the *IGK* intronic enhancer (Ei), whereas rearrangement to one of the Vκ gene segments deletes the entire Jκ-Cκ area; both types of recombinations prevent expression of the *IGK* allele, and it is believed that such events participate in the regulation of allelic and $\kappa\lambda$ isotypic exclusion.

In addition, Feddersen et al. (7, 8) have described atypical *IGK* recombinations in virally transformed murine B cells and also in human B-lineage lymphoproliferations; this concerns rearrangements of the intronRSS heptamer to the RSS of one of the Jκ segments (JκRSS-intronRSS signal joint) and rearrangements of a Vκ gene segment to the intronRSS (Vκ-intronRSS recombinations). Furthermore, JκRSS-Kde rearrangements have been identified in a case of human acute leukemia (9). The effects of these so-called atypical *IGK* rearrangements are versatile. Vκ-intronRSS rearrangements result in deletion of the entire Jκ gene segment cluster and the Cκ exon is removed upon JκRSS-Kde recombination. In contrast, in case of downstream JκRSS-intronRSS rearrangement, functional expression of the upstream Vκ-Jκ on the same allele could still be possible. Only if the JκRSS-intronRSS recombination involves the Jκ1RSS, a functional Ig κ-chain can no longer be formed, as no Jκ segments are then available for Vκ-Jκ recombination.

Based on extensive Southern blot and PCR screening, we identified a series of human B cell malignancies with uncommon *IGK* locus hybridization patterns and/or extended PCR product sizes, suspicious of the presence of the before mentioned atypical *IGK* gene rearrangements. These malignancies constitute single-cell

*Department of Immunology, Erasmus MC, University Medical Center Rotterdam, Rotterdam, The Netherlands; and †Department of Internal Medicine I, Division of Hematology, University of Vienna, Vienna, Austria

Received for publication March 3, 2004. Accepted for publication July 13, 2004.

The costs of publication of this article were defrayed in part by the payment of page charges. This article must therefore be hereby marked *advertisement* in accordance with 18 U.S.C. Section 1734 solely to indicate this fact.

[1] A.W.L. was supported by the Haak-Bastiaanse Kuneman Foundation; and U.J. and B.N. were supported by the Center of Molecular Medicine of the Austrian Academy of Sciences Grant 20010.

[2] Address correspondence and reprint requests to Dr. Anton W. Langerak, Molecular Immunology Unit, Department of Immunology, Erasmus MC, University Medical Center Rotterdam, Dr. Molewaterplein 50, 3015 GE, Rotterdam, The Netherlands. E-mail address: a.langerak@erasmusmc.nl

[3] Abbreviations used in this paper: *IGH*, Ig H chain locus; *IGK*, Igκ locus; *IGL*, Igλ locus; Kde, κ-deleting element; ALL, acute lymphoblastic leukemia; AML, acute myeloid leukemia; BM, bone marrow; CAT, chloramphenicol acetyltransferase; CLL, chronic lymphocytic leukemia; MNC, mononuclear cells; PB, peripheral blood; RQ-PCR, real-time quantitative PCR; RSS, recombination signal sequence.

0022-1767/04/$02.00

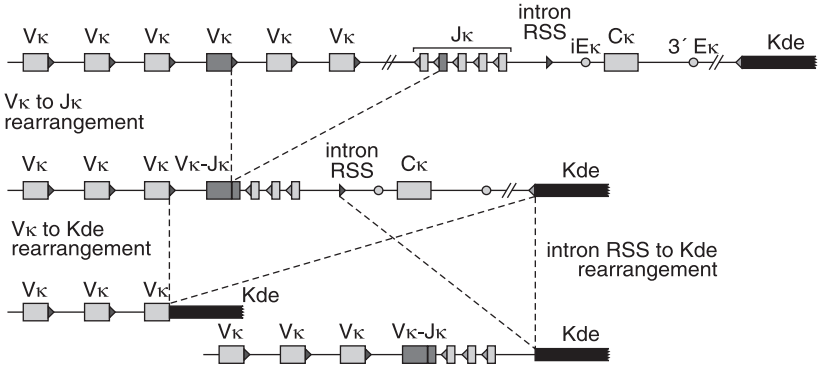

FIGURE 1. Schematic overview of classical rearrangements in the human *IGK* locus. *IGK* recombination mostly starts with a Vκ-Jκ rearrangement. The functionality of this rearrangement can be disrupted by rearrangement of the Kde. Recombination of Kde to an isolated heptamer in the intron between the Jκ and Cκ segments (intron-Kde rearrangement) results in deletion of the Cκ region, whereas recombination between Kde and a Vκ gene segment deletes the entire (Vκ) Jκ-Cκ region. Both types of Kde rearrangements also result in deletion of the *IGK* enhancers (iEκ and 3′Eκ), probably precluding further rearrangements in the human *IGK* locus.

model systems that enable the study of atypical *IGK* recombinations in full detail, i.e., within the context of the entire *IGK*/*IGL* L chain gene configuration. More importantly, we also analyzed and quantified the occurrence of these *IGK* recombinations in normal human peripheral blood and tonsillar B lymphocytes. The analysis of intermediate circular excision products, as well as functional data obtained in recombination substrate assays, allowed us to investigate whether specific rearrangements are formed via single-step or multistep rearrangements. Based on these data, we now propose a comprehensive and integrated model of the step-wise consecutive recombinations in the human *IGK* locus, including the here-described atypical *IGK* recombinations. The implications of these recombination pathways on Igκ protein expression and allelic exclusion of human *IGK* genes are discussed.

Materials and Methods

Cell samples

Several leukemia/lymphoma cell samples were selected on the basis of an initial suspicion of atypically rearranged *IGK* genes, as deduced from initial Southern blot hybridization patterns and/or extended PCR product sizes (10). These included the precursor B cell lines 380 and RCH-ACV, bone marrow (BM), or lymph node samples from precursor B cell acute lymphoblastic leukemia (precursor B-ALL; $n = 5$), B cell non-Hodgkin's lymphoma ($n = 4$), B cell chronic lymphocytic leukemia (B-CLL; $n = 2$), one unclassified B cell proliferation, and an acute myeloid leukemia (AML-M5) showing illegitimate atypical *IGK* recombination. BM mononuclear cells (MNC) were isolated by Ficoll-Paque (density, 1.077 g/ml; Amersham Biosciences, Buckinghamshire, U.K.) density centrifugation. BM-MNC fractions and lymph node suspensions were subsequently used for DNA and RNA isolation. Tonsils, peripheral blood (PB)-MNC, and (regenerating) BM-MNC from healthy controls were included as a source of normal B lymphocytes.

DNA isolation and Southern blot analysis

DNA isolation and Southern blot analysis was performed as previously described (11). In short, 15–20 μg genomic DNA was digested with restriction enzymes, separated in 0.7% agarose gels, and vacuum blotted. The configuration of the *IGK* locus was determined using *Bgl*II and *Bam*HI/*Hin*dIII digests and ^{32}P-labeled probes specific for the areas upstream (IGKJU) or downstream (IGKJ5) of the Jκ segments, or specific for the Cκ (IGKC) and the Kde (IGKDE) regions (10). *IGL* rearrangements were studied in *Eco*RI/*Hin*dIII digests using a general *IGL* probe (IGLC3) or probes specific for the Jλ1-Cλ1 (IGLC1D) or Jλ2-Cλ2 and Jλ3-Cλ3 (IGLJ2) areas in combination with *Bgl*II digests (12, 13).

Primer design

To detect recombinations between JκRSS elements and the intronRSS heptamer, new primer sets were designed (Fig. 2, and Table I). Using the germline *IGK* sequence (accession no. X67858) and OLIGO 6.2 software, a Jκ consensus primer (Jκ2-5-F1-EMC) was designed to detect rearrangements between Jκ2RSS, Jκ3RSS, Jκ4RSS, or Jκ5RSS and the intronRSS. The Jκ2-5-F1-EMC primer recognizes a homologous sequence in each Jκ gene segment upstream of the JκRSS that rearranges to intronRSS. To detect Jκ1RSS rearrangements a separate primer was designed that recognizes a sequence upstream of Jκ1 (Jκ1-F1-EMC). A primer downstream of intronRSS (intron-R1-EMC) was chosen as reverse primer. JκRSS-Kde recombinations were analyzed using the Jκ1-F1-EMC and Jκ2-5-F1-EMC primers together with a Kde primer. For detection of Vκ-intronRSS rearrangements, Vκ family primers as well as a Vκ consensus primer were used in combination with the earlier mentioned intron-R1-EMC primer (Fig. 2, and Table I). Inversional Vκ-intronRSS rearrangements were analyzed using the same Vκ family primers, in combination with a primer recognizing a sequence upstream of intronRSS (intronRSS primer) (Fig. 2, and Table I).

To specifically analyze circular excision products that are uniquely formed during JκRSS-intronRSS recombination, primers recognizing the Jκ segments (Jκ1-4) and the area upstream of intronRSS (intronRSS primer) were used (Fig. 2, and Table I) (14).

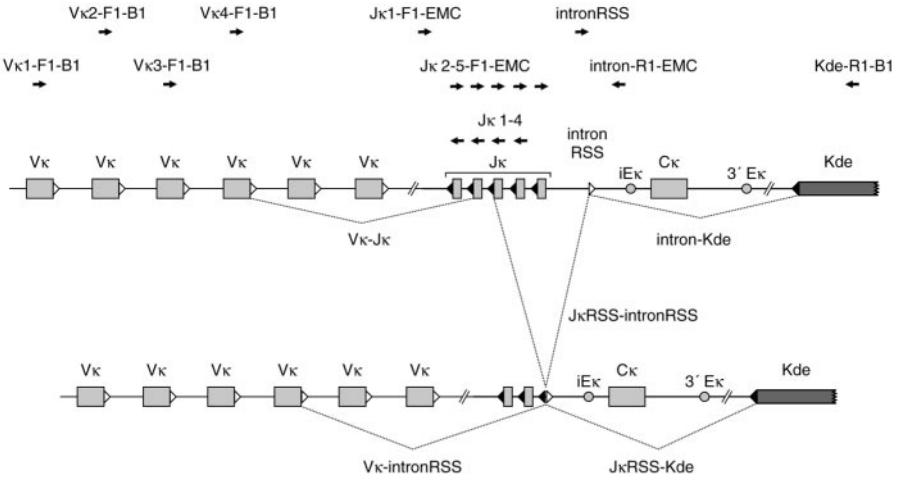

FIGURE 2. Schematic diagram of primer sets for detection of atypical *IGK* gene rearrangements such as JκRSS-intronRSS, Vκ-intronRSS and JκRSS-Kde rearrangements. Approximate position of the specially designed primers is indicated; the sequences of the primers are given in Table I. Classical *IGK* rearrangements as well as atypical JκRSS-intronRSS, Vκ-intronRSS, and JκRSS-Kde rearrangements are shown schematically.

Table I. *Oligonucleotides*

Oligonucleotide	Primer Probe	Sequence (5′ → 3′)	Reference
Rearrangement PCR			
Vκ1-F1-B1	Forward	GTAGGAGACAGAGTCACCATCACT	27
Vκ2-F1-B1	Forward	TGGAGAGCCGGCCTCCATCTC	27
Vκ3-F1-B1	Forward	GGGAAAGAGCCACCCTCTCCTG	27
Vκ4-F1-B1	Forward	GGCGAGAGGGCCACCATCAAC	27
Vκcons[a]	Forward	GGTACCCAGTCTCCATCCTCCCTGTC	28
Jκ1-F1-EMC	Forward	GAAAGGAACCATCAGGCCATAGA	This study
Jκ2–5-F1-EMC	Forward	CCAAGGTGGAGATCAAACGTAAGT	This study
Intron-R1-EMC	Reverse	CCCCTAATGGAAATTTTCACTAAT	This study
Kde-R1-B1	Reverse	CCCTTCATAGACCCTTCAGGCAC	27
Circular excision product PCR			
Jκ1–4	Reverse	GTTACGTTTGATCTCCACCTTGGTCCC	14
IntronRSS	Forward	CGTGGCACCGCGAGCTGTAGAC	14
Recombination substrate assay			
Ckde (*Spe*I)	Forward	CCTCACTAGTGCCTCCCTTGAATAGTCC	This study
Kde-A (*Bgl*II)	Reverse	TCATAGATCTTTCAGGCACATGC	This study
Ki-1A (*Spe*I)	Forward	TCGAACTAGTGGCTTTGGTGGCCATG	This study
Ki-2B (*Bgl*II)	Reverse	TCTAAGATCTCAGTCTTCTCCCTG	This study
RQ-PCR			
Vκ1-F1-B1	Forward	GTAGGAGACAGAGTCACCATCACT	27
Jκ1-F2-EMC	Forward	AAGGGTTTCTGTTCAGCAAGACA	This study
Jκ4-F2-EMC	Forward	TCATATGATTGGCTTCAAGAGAGGT	This study
Intron-F1-B2	Forward	GGCACCGCGAGCTGTAGAC	This study
Jκ1-R1-EMC	Reverse	ACTGAGGAAGCAAAGTTTAAATTCTACTC	This study
Jκ4-R1-EMC	Reverse	CACAAAAACGCTCCAAATTTAAAAC	This study
Intron-R2-EMC	Reverse	CCCTGGTTTTCCCAGCTCA	This study
Kde-R2-B1	Reverse	TTCCTAGGGAGGTCAGACTC	27
T-Jκ1-EMC	TaqMan probe	CGGCCAAGGGACCAAGGTGGAA	This study
T-Jκ4-EMC	TaqMan probe	AGGGACCAAGGTGGAGATCAAACGTAAGTG	This study
T-intron-EMC	TaqMan probe	CAAATAATGCCACTAAGGGAAAGAGAACAGAAACGT	This study
T-Kde-cons1	TaqMan probe	AGCTGCATTTTTGCCATATCCACTATTTGGAGT	16

[a] cons, Consensus.

PCR analysis and sequencing

PCR amplification of JκRSS-intronRSS, Vκ-intronRSS, and JκRSS-Kde recombinations, as well as of inversional Vκ-intronRSS rearrangements and Jκ-intronRSS circular excision products was performed using the relevant primer sets (see *Primer design* and Table I). A 50-μl reaction volume contained 50 ng genomic DNA, 1.5 mM $MgCl_2$ (Applied Biosystems, Foster City, CA), 0.2 mM dNTP (Amersham Biosciences), 6.25 pmol of each primer, and 1 U of AmpliTaq Gold DNA polymerase in buffer II (Applied Biosystems). The PCR consisted of 10 min preactivation at 94°C, followed by 40 cycles of 45 s denaturation at 94°C, 90 s annealing at 60°C, and 2 min extension at 72°C, followed by 10 min final extension at 72°C. PCR products were electrophoresed on a 1% agarose gel and visualized with ethidium bromide.

After amplification, the PCR products were further analyzed by heteroduplex analysis to determine the monoclonal or polyclonal character (15). In short, following denaturation at 94°C for 5 min and reannealing at 4°C for 1 h, the PCR products were separated in 6% polyacrylamide gels in 0.5× Tris-boric acid-EDTA buffer.

PCR products derived from monoclonal rearrangements were directly sequenced. To sequence the polyclonal recombinations from tonsil and MNC samples from healthy controls, the PCR products were first cloned, using the pGEM-T Easy vector kit according to the manufacturer's instructions (Promega, Madison, WI). After transformation to competent cells, positive colonies were grown and plasmid DNA was isolated for further sequencing.

Sequencing was performed on the ABI 377 fluorescent sequencer (Applied Biosystems), using the dye terminator cycle sequencing kit and AmpliTaqFS DNA polymerase (Applied Biosystems). Sequencing primers were identical with those used for PCR amplification. Sequencing was performed using either 60 ng of monoclonal PCR product and 3.2 pmol primer, or 500 ng of plasmid DNA with cloned PCR products from healthy controls and 6 pmol primer, in combination with 5 μl of dye terminator mix. The cycling protocol consisted of 25 cycles of 30 s, 96°C, followed by 4 min, 60°C.

Analysis of the obtained sequences was performed using the germline *IGK* genomic sequence (accession no. X67858). Vκ and Jκ gene segments were identified using DNAPLOT software (W. Müller and H.-H. Althaus, University of Cologne, Cologne, Germany) by searching for homology with all known human germline *IGK* sequences obtained from the VBASE directory of human Ig genes (http://www.mrc-cpe.cam.ac.uk/imt-doc/) and/or ImmunoGenetics (IMGT) (http://imgt.cines.fr:8104).

Real-time quantitative PCR (RQ-PCR) analysis of different types of IGK *gene recombinations*

RQ-PCR of different *IGK* recombinations was essentially performed as described previously using ABI Prism 7700 equipment (Applied Biosystems) (16). As clonal control DNA for the analyzed *IGK* recombinations, the following sources with high percentages (90–100%) of clonal cells were selected: cell line U698 (Vκ1-Jκ1), a B-CLL sample (Vκ1-Jκ4), cell line ROS15 (Vκ1-Kde), cell line Nalm1 (intron-Kde), B-CLL sample 91-062 (Jκ1RSS-intronRSS), ALL sample 5381 (Jκ4RSS-intronRSS), cell line RCH-ACV (Vκ1-intronRSS), and AML sample 95-058 (Jκ4RSS-Kde); no clonal control DNA was available for Jκ1RSS-Kde. The applied forward/reverse primers and TaqMan probes are listed in Table I.

All control cell lines and leukemic DNA samples were serially diluted in HeLa DNA as nontemplate control. A standard albumin RQ-PCR was performed to normalize the amount of input DNA of the nondiluted control DNA and DNA from tonsil, PB-MNC, and (regenerating) BM-MNC using serially diluted reference buffy DNA. In a typical 25-μl RQ-PCR, 5 μl of genomic DNA (20 ng/μl), 12.5 μl of 2× master mix, 22.5 pmol specific forward primer, 22.5 pmol specific reverse primer, and 2.5 pmol specific TaqMan probe were used. In two independent experiments, reactions were always performed in duplo. The protocol consisted of 2 min at 50°C and 10 min at 95°C, followed by 50 cycles of 15 s at 95°C and 1 min at 60°C. Ten-fold serial dilutions of each clonal control DNA (500–0.5 ng of template DNA) were used to make a standard curve for that particular type of *IGK* recombination RQ-PCR. C_T values of tonsil, PB-MNC, and BM-MNC DNA for a particular *IGK* RQ-PCR were subsequently plotted on the respective standard curve, and expressed as percentage recombination relative to the respective clonal control DNA.

Recombination substrate assay

The recombination substrate assay was essentially performed as described previously (17). In short, recombination plasmids with the chloramphenicol acetyltransferase (CAT) gene under control of the Ptac promoter were

used; in these constructs, CAT expression is prevented by a termination signal (OOP) upstream of the CAT coding sequence (see also Fig. 5 for further explanation). In eukaryotic cells, recombination between sequences in the upstream and downstream cassettes, which flank the OOP termination signal, results in removal of the latter, thereby giving rise to CAT expression when transformed in *Escherichia coli*. Cassettes for analysis of human *IGK* RSS-like elements (see also Fig. 5) were obtained by PCR amplification from genomic DNA, using specific primers with specific restriction sites (*Mlu*I and *Sal*I or *Not*I for the upstream cassette; *Spe*I and *Bgl*II for the downstream cassette) for easy cloning into the recombination backbone vector: (*Mlu*I)-Vκ A2/2D-29-(*Not*I)-Vκ A27/3-20-(*Sal*I)//(*Spe*I)-Jκ1-(*Bgl*II) (17). Primers used for constructing the various cassettes are listed in Table I. Cloning of the intron RSS motif cassette was performed as follows: PCR amplification on DNA from cells with germline *IGK* genes using Ki-1A (*Spe*I) and Ki-2B (*Bgl*II) primers, subcloning in pPCR-Script AmpSK(+) (Stratagene, La Jolla, CA) in the correct orientation, and finally digestion with *Not*I/*Sal*I and further cloning using *Not*I and *Sal*I restriction sites into the appropriate recombination substrates. The Kde cassette was produced by PCR amplification of germline *IGK* DNA using CKde (*Spe*I) and Kde-A (*Bgl*II) primers, and subsequently cloned via *Spe*I and *Bgl*II restriction sites into the appropriate recombination substrates. Finally, to produce the signal joint cassettes, the Jκ1RSS-intronRSS and Jκ3RSS-intronRSS signal joints were PCR amplified from leukemic cells harboring these elements using primers Jκ1-F1-EMC or Jκ2-5-F1-EMC together with intron-R1-EMC. PCR products were subcloned in pPCR-Script AmpSK(+), and taken out *Bss*HI/*Not*I. Because *Bss*HI has a compatible overhang with *Mlu*I, the fragment could directly be cloned as an *Mlu*I/*Not*I cassette into the appropriate recombination substrates.

Following transient transfection of recombination constructs into 18.8 Abelson's murine leukemia virus transformed murine precursor B-cells, plasmids (recombined and intact) were recovered after 48 h. Plasmids were subsequently transformed into *E. coli*, which were further cultured on ampicillin (50 μg/ml) and chloramphenicol (5 μg/ml). Recombined plasmid DNA was then isolated from resulting chloramphenicol-selected colonies and PCR-amplified using specific primers for the upstream and downstream sequences, followed by direct sequencing for identification of exact recombination breakpoints.

Results

Atypical IGK *recombinations detected in human B-lineage lymphoproliferations*

In the process of screening human B cell lymphoproliferations by *IGK* Southern blot and PCR analysis, we have come across cases with *IGK* recombinations other than the classical Vκ-Jκ, Vκ-Kde, and/or intron-Kde joinings (Fig. 1). These atypical *IGK* recombinations were further studied by Southern blot analysis using four different probes to determine the exact configuration of both *IGK* alleles (Fig. 3, and Table II).

In two samples (91-062 and F-7), rearranged bands of equal size were seen upon hybridization with the IGKJU and IGKC probes, which were interpreted as JκRSS-intronRSS rearrangements. Several other samples (4882, 94-101, 95-060, G-10, 4511, 5301, 95-074, and cell line RCH-ACV) showed a rearranged band using the IGKC probe with concomitant deletion of IGKJU and/or IGKJ5 hybridization signal, suggestive of a Vκ-intronRSS recombination. One case (5381) showed two nonidentically rearranged bands upon IGKJU and IGKC hybridization and loss of IGKJ5 signal, which most likely fits with an inversional rearrangement between a Vκ segment from the distal (inverted) cluster and a Jκ segment in combination with a JκRSS-intronRSS rearrangement on the same allele. Finally, in four samples (92-051, 5712, 95-058, and cell line 380), a rearranged band was seen upon IGKDE hybridization with parallel loss of IGKJU, IGKJ5, and IGKC hybridization signal, which might be explained by a true Vκ-Kde rearrangement or by a variant type Vκ-Jκ and JκRSS-Kde rearrangement (see later).

Because deletional rearrangements in the *IGK* locus mostly coincide with *IGL* gene rearrangements, we also checked this coincidental occurrence for atypical *IGK* recombinations. In 8 of the 13 cases, both *IGL* alleles were in germline configuration. Of the five cases showing *IGL* rearrangements (Table II), three contained at least one classical Kde recombination; in the other two (4511 and 5301), Vκ-intronRSS rearrangements were observed. However, because other cases (among others, case 95-074 and cell line RCH-ACV) displayed isolated Vκ-intronRSS recombinations without Vλ-Jλ rearrangements, a complete association between atypical *IGK* recombinations and the start of *IGL* gene recombination seems unlikely.

Detailed characterization of the detected atypical IGK *recombinations*

The vast majority of Southern blot deduced atypical *IGK* rearrangements could be confirmed via PCR heteroduplex analysis and sequencing (Fig. 2, and Table II). The two JκRSS-intronRSS recombinations (91-062 and F-7) both involved Jκ1RSS. Of the many samples with presumed Vκ-intronRSS recombinations, only two indeed contained direct Vκ-intronRSS couplings (95-074 and cell line RCH-ACV). In six others (4882, 94-101, 95-060, G-10, 4511, and 5301), the unusually long Vκ-intronRSS PCR products cases revealed a Vκ-Jκ and JκRSS-intronRSS configuration. PCR and sequencing in sample 5381 further showed an inversional Vκ2D-28-Jκ3 rearrangement upstream of a Jκ4RSS-intronRSS coupling. Finally, in four other samples (92-051, 5712, 95-058, and cell line 380) the unusually long Vκ-Kde PCR products appeared to represent Vκ-Jκ and JκRSS-Kde rearrangements rather than direct Vκ-Kde couplings.

Remarkably, in most cases with Vκ-Jκ and JκRSS-intronRSS or Vκ-Jκ and JκRSS-Kde configurations neighboring Jκ segments

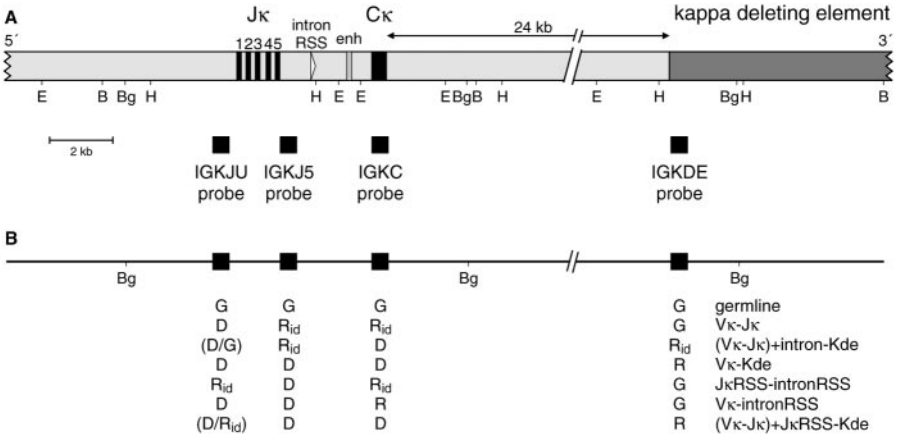

FIGURE 3. Southern blot analysis of human *IGK* gene rearrangements. *A*, Restriction map of part of the human *IGK* locus. The location of relevant *Bgl*II (Bg), *Bam*HI (B), *Eco*RI (E), and *Hin*dIII (H) restriction sites as well as the IGKJU, IGKJ5, IGKC, and IGKDE Southern blot probes are indicated. *B*, Example of interpretation of hybridization patterns of the complete set of *IGK* Southern blot probes in combination with *Bgl*II restriction digests.

Table II. *Complete configuration of* IGK *and* IGL *loci in human B-lineage lymphoproliferations with atypical* IGK *rearrangements*

		IGK					*IGL*	
		Allele with atypical *IGK* rearrangement				2nd *IGK* allele		
Case	Diagnosis/Classification[a]	Southern blotting pattern[b]	Configuration	Coupling[c]	Coupling[c] (frame)[d] upstream Vκ-Jκ	Configuration	Southern blotting pattern	Smlg
91–062	B-CLL	R_A/R_D	Jκ1RSS-intronRSS	Signal joint	n.a.	Vκ-Jκ + intron-Kde	R/R (V-J1/V-J3)	Igλ
F-7	B-NHL (DLCL)	R_A/R	Jκ1RSS-intronRSS	Signal joint	n.a.	Vκ-Jκ	G/G	ND
4882	Prec B-ALL (c-ALL)	R_A/G	Vκ2–30-Jκ1 + Jκ2RSS-intronRSS	−10 (3) −1	−3 (2) −2 (in)	Germline	G/G	n.a.
94–101	B-NHL (DLCL)	R_A/R	Vκ3–20-Jκ1 + Jκ2RSS-intronRSS	Signal joint	−3 (1) 0 (out)	Vκ-Jκ	G/G	Ig neg
95–060	B-NHL (DLCL)	R_A/R_D	Vκ1–39-Jκ2 + Jκ3RSS-intronRSS	Signal joint	0 (1) −2 (in)	Vκ-Jκ + intron-Kde	G/G	Igκ
G-10	Unclassified B-cell Proliferation	R_A/R	Vκ1–33-Jκ3 + Jκ4RSS-intronRSS	−4 (7) 0	−1 (7) −5 (out)	Vκ-Jκ	G/G	ND
4511	Prec B-ALL (c-ALL)	R_A/G	Vκ1–37-Jκ1 + Jκ4RSS-intronRSS	−2 (7) −6	0 (3) −2 (out)	Germline	R/G (Vλ-Jλ3)	n.a.
5301	Prec B-ALL (c-ALL)	R_A/R	Vκ1–39-Jκ2 + Jκ4RSS-intronRSS	−3 (5) −16	−3 (2) −1 (out)	Vκ-Jκ	R/G (Vλ-Jλ3)	n.a.
5381	Prec B-ALL (c-ALL)	R_A/G	Vκ2D-28-Jκ3 + Jκ4RSS-intronRSS[e]	0 (6) −1	−1 (3) −6 (out)	Germline	G/G	n.a.
RCH-ACV	Prec B-cell line	R_A/G	Vκ1–9-intronRSS	0 (15) −2	n.a.	Germline	G/G	n.a.
95–074	B-NHL (MALT/FL)	R_A/G	Vκ1–12-intronRSS	−1 (1) 0	n.a.	Germline	G/G	Igκ ?
380	Prec B-cell line	R_D/R_D	Vκ1–37-Jκ1 + Jκ2RSS-Kde	0 (8) −2	−2 (2) 0 (in)	Vκ-Jκ + intron-Kde	ND	n.a.
92–051	B-CLL	R_D/R_D	Vκ4–1-Jκ1 + Jκ2RSS-Kde	−2 (0) −14	−1 (0) −2 (in)	Vκ-Jκ + intron-Kde	R/G (Vλ-Jλ1)	Igλ
5712	Prec B-ALL (c-ALL)	$R_D/R_D/R_D$	Vκ4–1-Jκ2 + Jκ3RSS-Kde	0 (8) −4	0 (8) −6 (out)	trisomy: Vκ-Kde and Vκ-Jκ + intron-Kde	G/G	n.a.
95–058	AML-M5	R_D/G	Vκ3–20-Jκ3 + Jκ4RSS-Kde	0 (7) −3	0 (12) 0 (in)	Germline	R/G (Vλ-Jλ)	n.a.

[a] c-ALL, Common ALL; DLCL, diffuse large cell lymphoma; FL, follicular lymphoma; NHL, non-Hodgkin's lymphoma; prec, precursor.
[b] *IGK* Southern blotting pattern based on hybridization of *Bgl*II digests (+ *Bam*HI/*Hin*dIII and/or *Eco*RI for confirmation); G, germline; R, V-J rearrangement; R_A, atypical rearrangement; R_D, deletional rearrangement.
[c] Junctional region defined as 5′ deletion / insertion / 3′ deletion; signal joint: no deletion or insertion.
[d] In, In-frame; out, out-of-frame; n.a., not applicable.
[e] VκD, Vκ gene segment from the distal (inverted) cluster of Vκ gene segments.

were involved in the two couplings. Exceptions concerned 4511 and 5301 with V-Jκ1 and V-Jκ2, respectively, upstream of Jκ4RSS-intronRSS. All Jκ (except Jκ5) gene segments were found to be involved in the atypical *IGK* recombinations. Vκ segments in the upstream Vκ-Jκ couplings were derived from the three large Vκ families (Vκ1, Vκ2, Vκ3) and even concerned the most Jκ proximal Vκ4-1 segment. The few cases with direct Vκ-intronRSS couplings all concerned Vκ1 segments.

Detailed junctional region analysis revealed a signal joint configuration with two perfectly joined RSS elements in only four of the nine JκRSS-intronRSS atypical recombinations. The other five showed processed signal joints, i.e., nucleotide deletion from one or both RSS elements and even nucleotide insertion. Such a configuration is remarkable in view of the orientation of the JκRSS and intronRSS elements in the germline configuration, which in principle should lead to perfect signal joints. Coding jointlike configurations with deleted and inserted nucleotides were observed in all Vκ-intronRSS and JκRSS-Kde recombinations. Given their hybrid jointlike configuration, these were termed pseudohybrid joints. Analysis of Vκ-Jκ junctions upstream of JκRSS-intronRSS rearrangements revealed out-of-frame Vκ-Jκ fusions in five samples (94-101, G-10, 4511, 5301, and 5381), but in-frame alleles in two others (4882 and 95-060). Although no membrane Ig expression was observed (precursor B cell leukemia), in-frame Vκ2-30-Jκ1-Cκ transcripts were found to be present in case 4882 (data not shown). In 95-060, membrane Igκ protein expression was observed that could only result from the Vκ1-39-Jκ2 and Jκ3RSS-intronRSS allele, because the other allele contained a deletional rearrangement. Hence, the presence of a JκRSS-intronRSS recombination (except for Jκ1RSS-intronRSS) does not seem to block expression of an in-frame upstream Vκ-Jκ rearrangement.

Occurrence of atypical IGK *recombinations in normal human B cells*

To exclude that the atypical *IGK* rearrangements are only formed aberrantly in leukemic cells or (virally) transformed cells, tonsillar DNA from a healthy individual was analyzed. Using the same *IGK* primers as for the clonal cell samples, the tonsillar DNA was amplified and per type of rearrangement 5–15 cloned PCR products were sequenced (Table III). Vκ-intronRSS and JκRSS-intronRSS sequences both could readily be amplified. Many of the Vκ-intronRSS recombinations concerned couplings with heterogeneous Vκ segment usage and showed pseudohybrid joints with a comparable extent of nucleotide deletion and insertion as seen in the clonal cell samples. Part of the seemingly Vκ-intronRSS recombinations in tonsillar DNA actually concerned Vκ-Jκ and JκRSS-intronRSS configurations with heterogeneous Vκ family and Jκ gene segment usage. Interestingly, in contrast to the clonal cell samples, the vast majority (11/13 sequences) of tonsillar JκRSS-intronRSS rearrangements displayed perfect signal joints. Finally, heterogeneous (i.e., diverse with deletion and insertion of nucleotides) JκRSS-Kde recombinations could also be identified in tonsillar B cells, though the Jκ usage seemed to be less diverse in the small number of sequences analyzed in detail. Taken together, these data suggest that the atypical *IGK* recombinations that we initially identified in transformed cell samples do represent physiological events given their occurrence in healthy control tonsillar B cells.

Quantitation of IGK *recombinations by RQ-PCR analysis*

RQ-PCR was applied to quantify the different types of *IGK* recombinations in (regenerating) BM-MNC, PB-MNC, and tonsil. For this purpose Vκ1, Jκ1(RSS), Jκ4(RSS), Kde, and the intronRSS heptamer were chosen as representative elements

Table III. *Atypical* IGK *rearrangements and circular excision products as determined in healthy control tonsillar DNA*[a]

PCR Product	Coupling of Atypical Rearrangement[1]
JκRSS-intron RSS rearrangements	
Jκ1RSS - intronRSS	Signal joint
Jκ3RSS - intronRSS	Signal joint
Jκ3RSS - intronRSS	0/CTCCCCA/−1
Jκ4RSS - intronRSS	Signal joint
Jκ5RSS - intronRSS	Signal joint
Vκ1–12 - Jκ3 + Jκ4RSS - intronRSS	Signal joint
Vκ1–17 - Jκ3 + Jκ4RSS - intronRSS	Signal joint
Vκ2–26 - Jκ1 + Jκ2RSS - intronRSS	Signal joint
Vκ3D-7 - Jκ1 + Jκ2RSS - intronRSS	Signal joint
Vκ4–1 - Jκ3 + Jκ4RSS - intronRSS	Signal joint
Vκ5–2 - Jκ2 + Jκ3RSS - intronRSS	Signal joint
Vκ5–2 - Jκ3 + Jκ4RSS - intronRSS	Signal joint
Vκ5–2 - Jκ1 + Jκ2RSS - intronRSS	−10/C/0
Vκ - intronRSS rearrangements	
Vκ1–13 - intronRSS	−1/−/−4
Vκ1–27 - intronRSS	−2/T/−1
Vκ1–39 - intronRSS	−1/−/−4
Vκ2–18 - intronRSS	−3/CCTGGTGGGGAGG/−2
Vκ2–24 - intronRSS	−1/GAGGT/−4
Vκ3D-7 - intronRSS	−6/T/0
Vκ3–11 - intronRSS	−6/TC/−2
Vκ3–20 - intronRSS	−5/AAGGTG/−2
Vκ3D-20 - intronRSS	−2/A/−3
Vκ4–1 - intronRSS	−5/A/−3
Vκ4–1 - intronRSS	0/GG/−3
Vκ5–2 - intronRSS	−3/C/0
Vκ5–2 - intronRSS	0/TT/0
Vκ7–3 - intronRSS	−3/GCCG/−2
JκRSS - Kde rearrangements	
Jκ1RSS-Kde	−2/AG/−3
Jκ1RSS-Kde	−3/T/0
Jκ3RSS-Kde	−1/−/−3
Jκ3RSS-Kde	0/−/−4
Jκ - intron upstream circular excision products	
Jκ1 - intron upstream	0/GTGA/−3
Jκ1 - intron upstream	−4/−/ −2
Jκ1 - intron upstream	−4/GCCCAA/−8
Jκ2 - intron upstream	−2/A/−4
Jκ4 - intron upstream	0/GGAGG/−5
Jκ4 - intron upstream	−2/GTC/−2

[a] Junctional region defined as 5′ deletion/insertion of N nucleotides/3′ deletion.

involved in the various rearrangements. Following normalization of input DNA relative to an albumin standard curve, individual RQ-PCR were performed for these selected *IGK* recombination types. Using standard curves based on 10-fold serial dilutions of clonal control DNA samples, levels in tonsil, PB-MNC, and (regenerating) BM-MNC DNA were expressed as percentage recombination relative to the respective clonal control DNA. It is important to note that the various *IGK* recombination levels as measured in the normal tissues reflect relative and no absolute values, which formally cannot be used for direct comparisons between different types of recombinations in the human *IGK* locus. With this in mind, we nevertheless tried to roughly compare the frequencies of these different *IGK* recombinations (Table IV). In tonsil, intron-Kde rearrangements were most abundant and were arbitrarily set to 1.0; intron-Kde levels in PB and BM, being roughly 5- and 30-fold lower, respectively, than those observed in tonsil, were also set to 1.0. Vκ1-Jκ1, Vκ1-Jκ4, and Vκ1-Kde rearrangements appeared to be relatively frequent, with levels roughly 0.20−0.45 relative tothose of intron-Kde. Atypical Jκ1RSS-intronRSS and Jκ4RSS-intronRSS rearrangements could also be found in tonsil, PB, and BM, although the levels appeared to be much lower than those of the classical *IGK* rearrangements, ranging from (almost) undetectable to roughly 0.06 (as compared with intron-Kde levels) to maximally 0.1 (as compared with Vκ-Jκ and Vκ-Kde levels). Finally, recombination levels of the Vκ1-intronRSS and Jκ4RSS-Kde rearrangements were of the same order of magnitude as JκRSS-intronRSS. Due to the lack of a clonal control DNA sample, Jκ1RSS-Kde rearrangement levels could not be quantified; however, the C_T values were not that different from those obtained for Jκ4RSS-Kde rearrangements, suggesting a similar frequency for both rearrangements. Taken together, these data further confirm that atypical *IGK* rearrangements do indeed occur in BM, PB, and tonsillar B cells, albeit at frequencies of ~0.06 to 0.1 relative to the most abundant *IGK* gene rearrangements in these cells.

Excision circle analysis of atypical IGK *recombinations*

Next, we addressed the exact mechanism by which these atypical *IGK* recombinations are formed via detection of excision circles, which are formed during the rearrangement process. Because excision circles are not replicated upon further cell division, it is impossible to study these in clonally transformed cell samples. For that reason, we restricted our excision circle studies to tonsil DNA. Because virtually all JκRSS-intronRSS recombinations in tonsil DNA concerned perfect signal joints (Table III), it seemed logical

Table IV. *Relative levels of different types of* IGK *recombinations, as determined by RQ-PCR analysis*

Rearrangement	BM-MNC	PB-MNC	Tonsil
Intron-Kde[a]	1.0[a,b]	1.0[a,c]	1.0[a]
Vκ1-Jκ1	0.45 (0.39–0.50)	0.26 (0.22–0.29)	0.20 (0.18–0.22)
Vκ1-Jκ4	0.18 (0.15–0.20)	0.29 (0.24–0.33)	0.37 (0.25–0.51)
Vκ1-Kde	0.30 (0.20–0.39)	0.37 (0.24–0.50)	0.35 (0.20–0.45)
Jκ1RSS-intronRSS	0.06 (0.04–0.07)	0.02 (0.01–0.03)	0.03 (0.02–0.03)
Jκ4RSS-intronRSS	<0.01	<0.01	0.02 (0.01–0.04)
Vκ1-intronRSS	<0.01	<0.01	0.01 (0.01)
Jκ4RSS-Kde	<0.01	0.03 (0.02–0.04)	0.03 (0.02–0.03)

[a] Intron-Kde rearrangement levels, being most dominant, were arbitrarily set to 1, whereas other recombination levels are expressed relative to intron-Kde levels. Levels reflect average and ranges of at least two different experiments, each performed in duplo on the same DNA material.
[b] Intron-Kde rearrangement levels in BM-MNC were roughly 30-fold lower than in tonsil.
[c] Intron-Kde rearrangement levels in PB-MNC were roughly 5-fold lower than in tonsil.

to assume that excision circles would contain coding joints involving the Jκ gene segment and the region upstream of the intronRSS heptamer. Using a Jκ consensus primer as reverse primer in combination with a primer upstream of intronRSS as forward primer, PCR products can only be formed through amplification of such excision circles (Fig. 4*A*). Indeed, in tonsillar DNA, such Jκ-intron upstream PCR products could be identified (Fig. 4*B*, and Table III), strongly suggesting that JκRSS-intronRSS coupling occurs via direct recombination, resulting in a signal joint on the chromosome and a coding joint on the circular excision product.

The next question concerned the mechanism by which Vκ-intronRSS and JκRSS-Kde rearrangements are formed. Direct recombination would be less logical, as this would violate the 12/23 rule for at least the JκRSS-Kde recombination. Previously, it has been shown that in a signal joint, both RSS are functional and can undergo secondary rearrangements (18–20). Because most JκRSS-intronRSS signal joints in tonsil appeared to contain undamaged RSS elements, both RSS can be involved in continuing recombination processes leading to Vκ-intronRSS or JκRSS-Kde pseudohybrid joints. However, episomal circles formed by such secondary signal joint rearrangements are indistinguishable from normal Vκ-Jκ and intron-Kde rearrangements, because they use the same RSS and, therefore, generate the same signal joint excision product. Hence, it was impossible to design primers that would specifically recognize circular excision products resulting from Vκ-intronRSS and JκRSS-Kde recombinations.

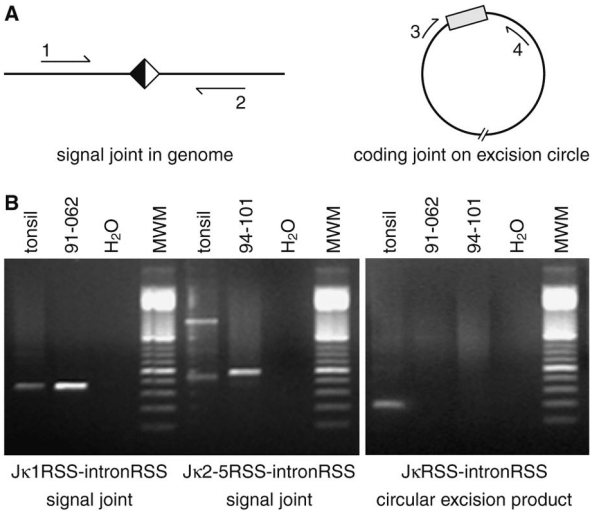

FIGURE 4. Atypical JκRSS-intronRSS recombination. *A*, Schematic drawing of a JκRSS-intronRSS signal joint as well as the parallel excision circle with the coding joint. Indicated are the primers that can be used for amplification of these signal and coding joints: 1, Jκ1-F1-EMC or Jκ2-5-F1-EMC; 2, intron-R1-EMC; 3, Jκ1-4; and 4, intronRSS (see also Fig. 2 and Table I). *B*, Agarose gel electrophoresis of PCR-amplified JκRSS-intronRSS signal joints and parallel coding joints with the primers as described in *A*.

Unraveling the mechanism of atypical IGK *recombination via recombination substrate assay*

To unravel the exact mechanism of Vκ-intronRSS and JκRSS-Kde recombinations, an in vitro recombination substrate assay was used. *IGK* RSS elements of interest together with their flanking sequences were cloned as upstream and downstream cassettes in a vector that contains an intermediate stop element for blocking CAT gene expression. Upon transfection in a precursor B cell line, proper recombination between RSS elements in the upstream and downstream cassettes results in removal of the stop element, thereby enabling CAT expression. Sequencing of colonies, selectively grown on chloramphenicol, allows determining the exact recombination breakpoints.

We first analyzed a construct in which the Jκ1 gene segment with its RSS was cloned in one cassette and the intronRSS heptamer with flanking DNA in the other (Fig. 5*A*). Sequence analysis revealed perfect signal joints between the Jκ1RSS and intronRSS elements, whereas analysis of the excision products showed fusion of the Jκ1 coding sequence and the upstream intron area with deletion as well as insertion of P and N nucleotides (Fig. 5*A*). This result nicely confirmed the observations from our excision circle analyses. We subsequently cloned the Jκ1RSS-intronRSS signal joint and flanking DNA from one of the leukemic cell samples, and tested it for its ability to recombine with the RSS of the frequently used VκA2/2D-29 and VκA27/3-20 gene segments (Fig. 5*B*), which was assumed to be the ongoing recombination step leading to Vκ-intronRSS pseudohybrid joint formation. Of the many colonies obtained in the assay, all 10 sequenced showed that V(D)J recombination between Vκ and the Jκ1RSS-intronRSS signal joint indeed occurs. Moreover, the sequences resembled the Vκ-intronRSS pseudohybrid joints as obtained from tonsil DNA, being diverse with deletion of nucleotides at both the Vκ and the signal joint sides as well as insertion of occasional N nucleotides and formation of P nucleotides (Fig. 5*B*). Finally, to test the functional properties of JκRSS-intronRSS signal joints in the other direction, we made a construct in which a Jκ3RSS-intronRSS signal joint was tested against the KdeRSS (Fig. 5*C*). Similarly, all sequenced constructs showed pseudohybrid joints. In all cases, Jκ3RSS was coupled to the Kde sequence, with diversity of deletion and insertion of both N and P nucleotides (Fig. 5*C*). Collectively, these results show that recombination between JκRSS and intronRSS

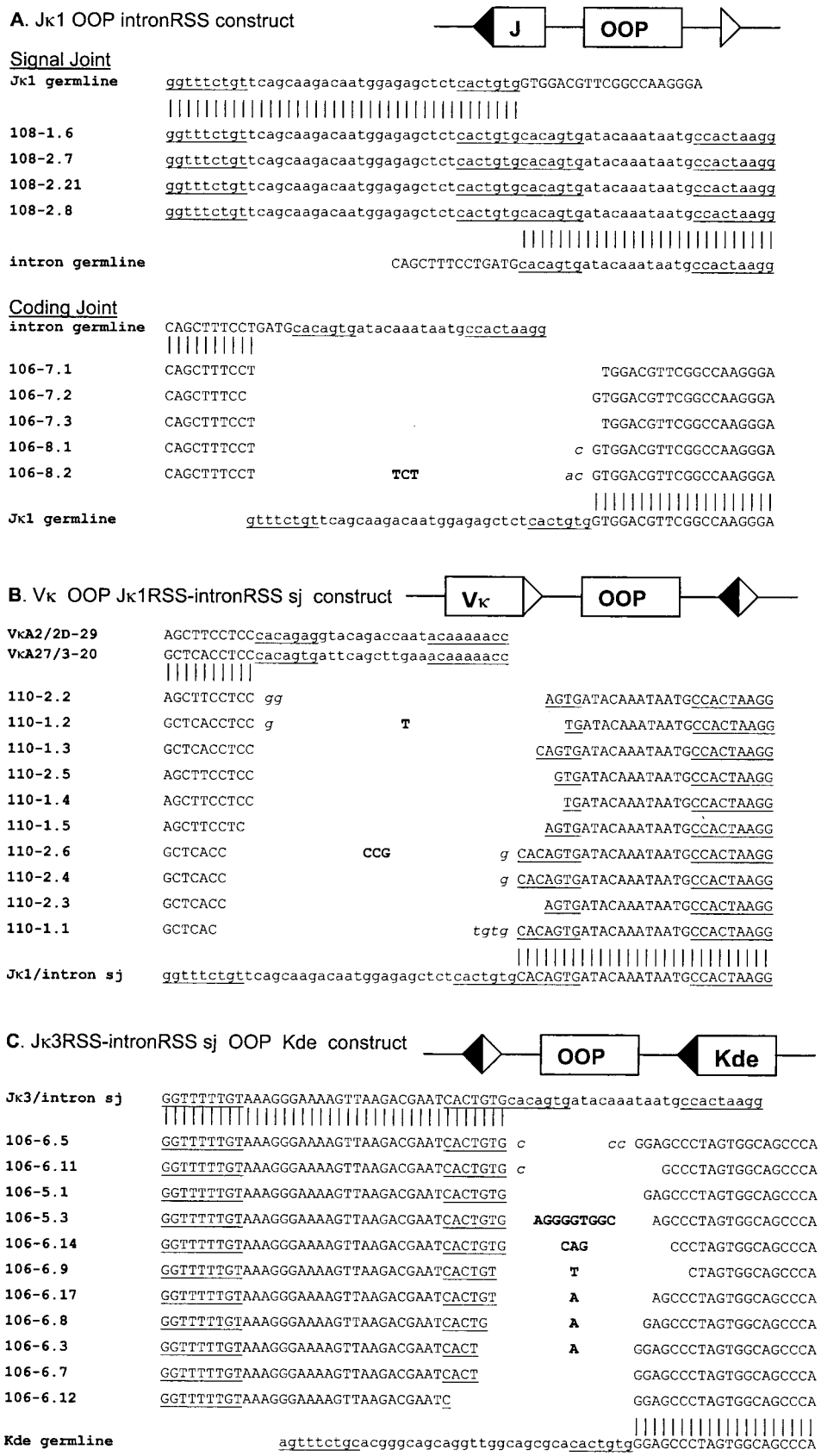

FIGURE 5. Recombination substrate assay. Sequences of clones obtained in recombination substrate assay, using different constructs (for a description see also *Materials and Methods*). *A*, Configurations of signal joints and coding joints formed upon recombination between the Jκ1 gene segment and the intronRSS heptamer. Perfect JκRSS-intronRSS signal joints are formed, whereas the coding joints show a variable level of deletion and insertion of nucleotides. *B*, Configurations of pseudohybrid joints formed upon recombination between VκA2/2D-29 or VκA27/3–20 and the Jκ1RSS-intronRSS signal joint, showing both deletion and insertion of nucleotides. *C*, Configurations of pseudohybrid joints formed upon recombination between the Jκ3RSS-intronRSS signal joint and Kde, with evidence for deletion and insertion of nucleotides.

leads to signal joint formation and that the composition and position of this signal joint is such that it can be involved in secondary recombination to either one of the Vκ gene segments or Kde, finally giving rise to Vκ-intronRSS and JκRSS-Kde pseudohybrid joints.

Discussion

The human *IGK* locus contains several RSS elements in addition to the RSS flanking Vκ and Jκ gene segments, allowing other rearrangements than the common V-J rearrangements to occur. Firstly, the presence of a 23-bp RSS flanking the Kde element at the very 3′ end of the locus provides an alternative partner for the 12-bp VκRSS elements, resulting in Vκ-Kde rearrangements. Secondly, the Kde element can also rearrange to an isolated heptamer in the Jκ-Cκ intron (intronRSS), resulting in intron-Kde rearrangements (Fig. 1). Thirdly, additional nonclassical recombinations involving VκRSS, JκRSS, intronRSS, and KdeRSS elements have been described by Feddersen et al. and Seriu et al. (7–9). Several of these rearrangements cannot be formed directly, either because of the inverted positions of their respective RSS (JκRSS and KdeRSS, and Vκ and intronRSS) or because their RSS spacer lengths do not obey the 12/23 rule (Jκ and Kde both contain RSS with 23-bp spacers). In this study, we describe the detailed characterization of three atypical JκRSS-intronRSS, Vκ-intronRSS, and JκRSS-Kde recombinations in human B cells and show how they fit in a scheme of sequential *IGK* recombinations.

Our data show that all three types of atypical rearrangements occur in B cell malignancies as well as in normal human tonsillar B cells. Semiquantitative analysis revealed that the classical Vκ-Jκ, Vκ-Kde, and intronRSS-Kde rearrangements are relatively frequent events, and that JκRSS-intronRSS and Vκ-intronRSS and JκRSS-Kde rearrangements are less predominant (<5% of intron-Kde rearrangement levels, and ~10% of the Vκ-Jκ and Vκ-Kde rearrangement levels) (Table IV). Based on this quantitation as well as the data from excision circle analysis and recombination substrate assays, a comprehensive and integrated model is proposed for the consecutive recombination events as they can occur in the *IGK* locus (Fig. 6). In this model, initial Vκ-Jκ recombination occurs once or multiple times until an in-frame combination is formed. If no in-frame rearrangement is obtained, two major inactivation pathways are available: 1) intron-Kde (Cκ deletion); or 2) Vκ-Kde (Jκ-Cκ deletion) recombination. Alternatively, in a minor pathway, JκRSS-intronRSS signal joints might be formed. Perfect JκRSS-intronRSS signal joints (i.e., without deleted nucleotides) can undergo subsequent rearrangement, either to an upstream RSS element of a Vκ segment (Vκ-intronRSS pseudohybrid joints) or to the downstream RSS of the Kde (JκRSS-Kde pseudohybrid joints). Finally, by analogy to intronRSS-Kde formation, ongoing recombination from Vκ-intronRSS rearrangements can theoretically result in Vκ-Kde recombinations, unless the intronRSS became damaged during the Vκ to JκRSS-intronRSS rearrangement. As this often proved to be the case (see Vκ-intronRSS pseudohybrid joint sequences in Table III), this recombination step is depicted with dotted lines in Fig. 6. We consider the possibility of ongoing recombination of JκRSS-Kde pseudohybrid joints into Vκ-Kde rearrangements not very likely either (dotted lines), because JκRSS-Kde couplings delete both enhancers (iEκ and 3′Eκ) that are known to be important for *IGK* recombination (21–23). Although Vκ-Kde rearrangements are very prominent, they thus probably are not end-stage rearrangements in each *IGK* inactivation pathway (see Fig. 6).

Though infrequent, formation of signal joints without coding joints in the genome, as in case of JκRSS-intronRSS couplings, has been observed before. For example, we previously reported on

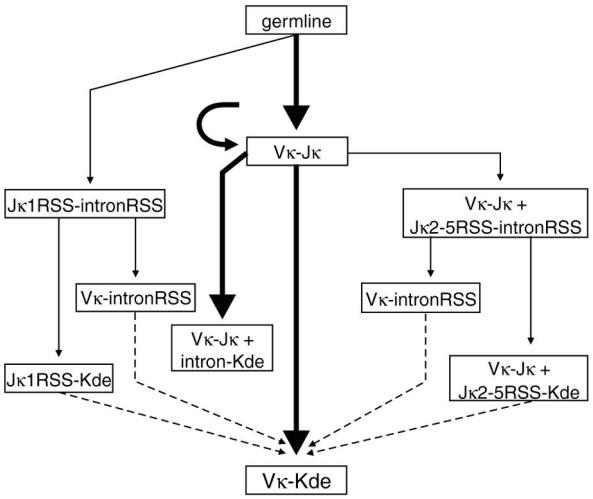

FIGURE 6. Tentative model describing the consecutive recombination events as they can occur in the human *IGK* locus. Starting from a germline allele, most recombination events concern Vκ-Jκ rearrangements, which in case no functional *IGK* allele can be expressed might be replaced by secondary Vκ-Jκ rearrangements, as long as upstream Vκ and downstream Jκ gene segments are available for recombination. Major consecutive rearrangements (thick lines) in the *IGK* locus are the classical Kde rearrangements: intron-Kde rearrangements downstream of a preserved Vκ-Jκ recombination, or Vκ-Kde rearrangements that loop out a pre-existing Vκ-Jκ coupling. Apart from these major classical rearrangements, also less frequent atypical rearrangements can occur. Recombination between any of the Jκ segments and the intronRSS results in JκRSS-intronRSS signal joints, which, except for the case that Jκ1RSS is involved, will be preceded by a Vκ-Jκ coupling. This signal joint, as shown in this study, can further recombine in two different ways: 1) recombination between a Vκ segment and a perfect JκRSS-intronRSS signal joint results in a Vκ-intronRSS coupling; and 2) recombination between Kde and a perfect JκRSS-intronRSS signal joint results in a JκRSS-Kde coupling. Finally, as long as the intronRSS of the Vκ-intronRSS pseudohybrid joint is still intact, further recombination to the RSS of Kde, leading to a Vκ-Kde coupling, might occur; however, because in many cases the intronRSS is actually damaged (see also sequences in Table III), this will often prevent further recombination, leaving the Vκ-intronRSS pseudohybrid joint as end-stage configuration. One might argue that in a similar way the undamaged JκRSS of a JκRSS-Kde coupling might still rearrange to the RSS of an upstream Vκ segment (as long as present); however, loss of both *IGK* enhancers in the (Vκ-Jκ) + JκRSS-Kde configuration implies that such a Vκ-Kde coupling most probably cannot be formed anymore, leaving the JκRSS-Kde pseudohybrid joints as end-stage configuration. For this reason, these latter recombination steps are presented as dotted lines.

the formation of Dδ2-Dδ3 signal joints in an experimental human epithelial model system upon transfection of E2A and the RAG proteins (24). These signal joints appeared to result from an alternative recombination mechanism leading to direct coupling of the upstream RSS of the Dδ2 segment and the downstream RSS of the Dδ3 segment (24). Similar signal joints were occasionally found in thymocytes. All of these Dδ2-Dδ3 signal joints concerned perfect couplings without deletion or N region insertion (24), which fits with the lack of N regions in most tonsillar JκRSS-intronRSS signal joints (80% of signal joints), but contrasts with the high frequency of imprecise JκRSS-intronRSS signal joints in B cell malignancies, particularly in precursor B-ALL. This unexpectedly high frequency of imprecise joints is probably caused by known continuous recombination activity in precursor B-ALL (25), resulting in further rearrangement of JκRSS-intronRSS couplings with perfect signal joints, but retention of the imprecise signal joints. Recently, we also found evidence for signal joint formation

as an intermediate step in the V(D)J-mediated oncogenic rearrangement in t (7, 9) in T-ALL (26). In thymocytes of healthy individuals, a signal joint configuration between the Dβ1RSS and a fortuitous RSS in the *TAL2* locus on chromosome 9 can occasionally be observed as a result of V(D)J-mediated translocation. Further rearrangement between this highly reactive signal joint intermediate and a Jβ2 segment would then result in *TAL2*RSS-Jβ2 hybrid joints as they are observed in T-ALL with t (7, 9) (26).

An important issue concerns the functional implications of the atypical *IGK* recombinations. When Jκ1RSS, being the most upstream JκRSS, is recombined to the intronRSS heptamer, Vκ-Jκ joints can no longer occur and hence no functional Igκ expression is possible from that allele. In that sense, Jκ1RSS-intronRSS recombinations function as deletional rearrangements. The same holds for Vκ-intronRSS and JκRSS-Kde rearrangements, which both most probably occur as secondary events following initial JκRSS-intronRSS signal joint formation. The lack of intact Jκ gene segments prohibits production of potentially functional Vκ-Jκ recombinations in *cis* in both cases. However, the functional implications are much less clear for Vκ-Jκ and Jκ2-5RSS-intronRSS recombinations. In theory, splicing of an upstream in-frame Vκ-Jκ exon to the Cκ exon could result in Igκ expression in such a configuration, unless the loss of important regulatory elements in the region between the Jκ segments and the intronRSS heptamer would prevent this. So far, human and mouse *IGK* enhancer sequences (iEκ) have only been identified in the 3′ part of the intron downstream of the intronRSS heptamer and not in the 5′ intron part (21–23). This is supported by our observation that JκRSS-intronRSS atypical joints did not block Vκ-Jκ-Cκ transcription and/or translation. Apparently, the initial occurrence of JκRSS-intronRSS signal joints (Jκ1RSS-intronRSS excluded) might be a simple side event of an active V(D)J recombinase system, but ongoing recombination to Vκ-intronRSS and JκRSS-Kde pseudohybrid joints leads to *IGK* allele inactivation.

In summary, in this study, we show that in addition to the dominant classical rearrangements in the human *IGK* locus (Vκ-Jκ, intron-Kde and Vκ-Kde), atypical *IGK* recombinations (JκRSS-intronRSS, Vκ-intronRSS, and JκRSS-Kde) also occur, albeit at frequencies of $<$5% of intron-Kde and $\sim$10% of Vκ-Jκ and Vκ-Kde (Table IV). As illustrated in the model (Fig. 6), initial Vκ-Jκ couplings can be followed by downstream JκRSS-intronRSS recombinations on the same allele. Because we could not identify functional implications of JκRSS-intronRSS couplings, we believe that such recombinations should be considered as occasional intermediates of an active V(D)J recombinase; Jκ1RSS-intronRSS recombinations are exceptional in that they do not allow functional Vκ-Jκ recombination and expression. Remarkably, in tonsils, the JκRSS-intronRSS couplings mostly, though not always, concerned perfect signal joints, whereas B cell malignancies (in particular precursor B-ALL) often showed damaged signal joints (Tables II and III). This can probably be explained by counterselection on perfect JκRSS-intronRSS signal joints for ongoing recombination in precursor B-ALL cells that are renowned for having a highly active V(D)J recombinase. Undamaged JκRSS-intronRSS signal joints are likely to undergo further recombination to Vκ-intronRSS or JκRSS-Kde pseudohybrid joints, as shown in recombination substrate assays (Fig. 5). The formation of both types of pseudohybrid joints might represent an alternative pathway of allele inactivation and allelic exclusion for those *IGK* alleles that have undergone initial aberrant recombinations: in case of Vκ-intronRSS recombination, no Jκ segments are left for functional *IGK* expression, while JκRSS-Kde recombination deletes the Cκ region and enhancers, thereby preventing expression of an Ig κ-chain. Theoretically, the Vκ-intronRSS pseudohybrid joint could be involved in further recombination to Kde (Vκ-Kde coupling). However, damaged intronRSS (see also Table III) frequently preclude this and consequently the Vκ-intronRSS pseudohybrid joint will often be the end-stage rearrangement (Fig. 6). Analogously, the undamaged JκRSS of a JκRSS-Kde coupling might theoretically rearrange to the RSS of an upstream Vκ segment, but the loss of both *IGK* enhancers in the (Vκ-Jκ) + JκRSS-Kde configuration probably blocks this, leaving the (Vκ-Jκ) + JκRSS-Kde rearrangement as end-stage configuration (Fig. 6). Although the usage of the here-described alternative *IGK* recombination pathway is limited, this pathway is essential for inactivation of *IGK* alleles with aberrant recombinations, which otherwise might hamper selection of functional Ig L chain proteins.

Acknowledgments

We thank members of the Molecular Immunology unit (Department of Immunology, Erasmus Medical Center) for stimulating discussions and valuable comments; V. H. J. van der Velden and M. van der Burg for critical reading of the manuscript; and the BIOMED-2 Concerted Action BMH4-CT98-3936 (coordinator J. J. M. van Dongen) for kindly providing two samples with atypical *IGK* recombinations for further analysis.

References

1. Ghia, P., E. ten Boekel, A. G. Rolink, and F. Melchers. 1998. B-cell development: a comparison between mouse and man. *Immunol. Today 19:480*.
2. Ghia, P., E. ten Boekel, E. Sanz, A. de la Hera, A. Rolink, and F. Melchers. 1996. Ordering of human bone marrow B lymphocyte precursors by single-cell polymerase chain reaction analyses of the rearrangement status of the immunoglobulin H and L chain gene loci. *J. Exp. Med. 184:2217*.
3. Gorman, J. R., and F. W. Alt. 1998. Regulation of immunoglobulin light chain isotype expression. *Adv. Immunol. 69:113*.
4. Van der Burg, M., T. Tumkaya, M. Boerma, S. de Bruin-Versteeg, A. W. Langerak, and J. J. van Dongen. 2001. Ordered recombination of immunoglobulin light chain genes occurs at the IGK locus but seems less strict at the IGL locus. *Blood 97:1001*.
5. Korsmeyer, S. J., P. A. Hieter, J. V. Ravetch, D. G. Poplack, T. A. Waldmann, and P. Leder. 1981. Developmental hierarchy of immunoglobulin gene rearrangements in human leukemic pre-B-cells. *Proc. Natl. Acad. Sci. USA 78:7096*.
6. Siminovitch, K. A., A. Bakhshi, P. Goldman, and S. J. Korsmeyer. 1985. A uniform deleting element mediates the loss of κ genes in human B cells. *Nature 316:260*.
7. Feddersen, R. M., D. J. Martin, and B. G. Van Ness. 1990. Novel recombinations of the IGκ-locus that result in allelic exclusion. *J. Immunol. 145:745*.
8. Feddersen, R. M., D. J. Martin, and B. G. Van Ness. 1990. The frequency of multiple recombination events occurring at the human Igκ L chain locus. *J. Immunol. 144:1088*.
9. Seriu, T., T. E. Hansen-Hagge, Y. Stark, and C. R. Bartram. 2000. Immunoglobulin κ gene rearrangements between the κ deleting element and Jκ recombination signal sequences in acute lymphoblastic leukemia and normal hematopoiesis. *Leukemia 14:671*.
10. Beishuizen, A., M.-A. J. Verhoeven, E. J. Mol, and J. J. M. Van Dongen. 1994. Detection of immunoglobulin κ light chain gene rearrangement patterns by Southern blot analysis. *Leukemia 8:2228*.
11. Van Dongen, J. J. M., and I. L. M. Wolvers-Tettero. 1991. Analysis of immunoglobulin and T cell receptor genes. I. Basic and technical aspects. *Clin. Chim. Acta 198:1*.
12. Tumkaya, T., W. M. Comans-Bitter, M. A. Verhoeven, and J. J. van Dongen. 1995. Southern blot detection of immunoglobulin λ light chain gene rearrangements for clonality studies. *Leukemia 9:2127*.
13. Tümkaya, T., A. Beishuizen, I. L. M. Wolvers-Tettero, and J. J. M. Van Dongen. 1996. Identification of immunoglobulin λ isotype gene rearrangements by Southern blot analysis. *Leukemia 10:1834*.
14. Van Dongen, J. J. M., A. W. Langerak, M. Bruggemann, P. A. S. Evans, M. Hummel, F. L. Lavender, E. Delabesse, F. Davi, E. Schuuring, R. Garcia-Sanz, et al. 2003. Design and standardization of PCR primers and protocols for detection of clonal immunoglobulin and T-cell receptor gene recombinations in suspect lymphoproliferations: report of the BIOMED-2 Concerted Action BMH4-CT98-3936. *Leukemia 17:2257*.
15. Langerak, A. W., T. Szczepanski, M. Van der Burg, I. L. M. Wolvers-Tettero, and J. J. M. Van Dongen. 1997. Heteroduplex PCR analysis of rearranged T cell receptor genes for clonality assessment in suspect T cell proliferations. *Leukemia 11:2192*.
16. Van der Velden, V. H., M. J. Willemse, C. E. van der Schoot, K. Hahlen, E. R. van Wering, and J. J. van Dongen. 2002. Immunoglobulin κ deleting element rearrangements in precursor-B acute lymphoblastic leukemia are stable targets for detection of minimal residual disease by real-time quantitative PCR. *Leukemia 16:928*.
17. Marculescu, R., T. Le, P. Simon, U. Jaeger, and B. Nadel. 2002. V(D)J-mediated translocations in lymphoid neoplasms: a functional assessment of genomic instability by cryptic sites. *J. Exp. Med. 195:85*.

18. Hesse, J. E., M. R. Lieber, M. Gellert, and K. Mizuuchi. 1987. Extrachromosomal DNA substrates in pre-B cells undergo inversion or deletion at immunoglobulin V-(D)-J joining signals. *Cell 49:775*.
19. Lewis, S., A. Gifford, and D. Baltimore. 1984. Joining of Vκ to Jκ gene segments in a retroviral vector introduced into lymphoid cells. *Nature 308:425*.
20. Lewis, S., A. Gifford, and D. Baltimore. 1985. DNA elements are asymmetrically joined during the site-specific recombination of κ immunoglobulin genes. *Science 228:677*.
21. Xu, Y., L. Davidson, F. W. Alt, and D. Baltimore. 1996. Deletion of the Igκ light chain intronic enhancer/matrix attachment region impairs but does not abolish Vκ Jκ rearrangement. *Immunity 4:377*.
22. Mostoslavsky, R., N. Singh, A. Kirillov, R. Pelanda, H. Cedar, A. Chess, and Y. Bergman. 1998. κ-chain monoallelic demethylation and the establishment of allelic exclusion. *Genes Dev. 12:1801*.
23. Inlay, M., F. W. Alt, D. Baltimore, and Y. Xu. 2002. Essential roles of the κ light chain intronic enhancer and 3′ enhancer in κ rearrangement and demethylation. *Nat. Immunol. 3:463*.
24. Langerak, A. W., I. L. Wolvers-Tettero, E. J. van Gastel-Mol, M. E. Oud, and J. J. van Dongen. 2001. Basic helix-loop-helix proteins E2A and HEB induce immature T-cell receptor rearrangements in nonlymphoid cells. *Blood 98:2456*.
25. Szczepanski, T., M. J. Pongers-Willemse, A. W. Langerak, and J. J. van Dongen. 1999. Unusual immunoglobulin and T-cell receptor gene rearrangement patterns in acute lymphoblastic leukemias. *Curr. Top. Microbiol. Immunol. 246:205*.
26. Marculescu, R., K. Vanura, T. Le, P. Simon, U. Jager, and B. Nadel. 2003. Distinct t(7;9)(q34;q32) breakpoints in healthy individuals and individuals with T-ALL. *Nat. Genet. 33:342*.
27. Pongers-Willemse, M. J., T. Seriu, F. Stolz, E. d'Aniello, P. Gameiro, P. Pisa, M. Gonzalez, C. R. Bartram, E. R. Panzer-Gruemayer, A. Biondi, et al. 1999. Primers and protocols for standardized detection of minimal residual disease in acute lymphoblastic leukemia using immunoglobulin and T cell receptor gene rearrangements and *TAL1* deletions as PCR targets: report of the BIOMED-1 Concerted Action: investigation of minimal residual disease in acute leukemia. *Leukemia 13:110*.
28. Feeney, A. J., G. Lugo, and G. Escuro. 1997. Human cord blood κ repertoire. *J. Immunol. 158:3761*.